Fibers and Polymers 2016, Vol.17, No.8, 1262-1268
DOI 10.1007/s12221-016-6306-1

ISSN 1229-9197 (print version)
ISSN 1875-0052 (electronic version)

Fracture Behavior of PAN-based Carbon Fiber Tow in a Chopping Process on an Elastic Support

Yingxi Xie[1,2], Longsheng Lu[1,2]*, Zhaorui Hou[1], Yong Tang[1], Limei Miao[1], and Xiaokang Liu[1]

[1]*School of Mechanical & Automotive Engineering, South China University of Technology, Guangzhou 510640, China*
[2]*Department of Mechanical Engineering, University of California, Berkeley 94720, United States*
(Received March 7, 2016; Revised July 13, 2016; Accepted July 22, 2016)

Abstract: As useful composite reinforcements, chopped carbon fibers are usually manufactured by elastic support-based chopping technologies, such as radial chopping technology. In this paper, the fracture behavior of a polyacrylonitrile (PAN)-based carbon fiber tow being chopped on an elastic support was analyzed. The fracture behavior and failure mode of the chopped carbon fiber tow were tested and discussed. Due to that the failure mode of a carbon fiber being chopped on an elastic support is flexural fracture, some interesting properties are appeared in the chopping process of PAN-based CF tow, such as robustness of the blade edge radius and failure order of the tow.

Keywords: Carbon fiber, Fracture behavior, Chop, Elastic support, Robustness

Introduction

Carbon fibers (CFs) are ideal reinforcements for high-performance composites. As indicated by Frank *et al.* [1], CFs have the outstanding properties of high specific strength, high specific modulus, high resistance to fatigue and creep, excellent electrical and thermal conductivity, strong chemical inertness, exceptional thermo-physical properties and excellent damping characteristics. Thus far, CFs are widely applied in the aviation, spaceflight, automobile, electronic, machinery, chemical, sports equipment and other fields. Generally, in reinforced composites, CFs can be used in the shapes of continuous or short pieces (known as chopped CFs) with a length of several millimeters. Compared with continuous CFs, the chopped CFs are easier to make reinforced composites because of their convenient post-processing property. Dong *et al.* [2] used a simple poured molding method to fabricate chopped CF/epoxy resin composites and concluded that the fracture toughness was improved significantly compared with that of pure epoxy resins. Wang *et al*. [3] developed a chopped CF/cement composite using a pure molding method and discovered that the electromagnetic wave absorbability was enhanced. Ahmad *et al*. [4] used a powder injection mold technology to create orientation chopped CF/aluminum composites. Moreover, Karsli *et al*. [5] and Ozkan *et al*. [6] successfully applied extrusion technology to produce chopped CF/polymer composites. On the whole, all of these composite fabrication methods acting on chopped CFs are low cost and can be easily scaled up. Additionally, chopped CFs can be used to form isotropous composites due to the random distribution mechanism. Therefore, 13 % of the world's CFs are used in the form of chopped CFs.

Generally, chopped CFs are produced through chopping continuous CFs into short pieces. Shen *et al.* [7] proposed a continuous processing method to manufacture chopped CFs, known as radial chopping technology. Figure 1(a) illustrates the schematic of the chopping process, in which an active rubber roller drives a press roller and a radial cutter to rotate under a certain pressure. Because of the friction between the rubber roller and the press roller, a fiber tow, which is a collection of continuous CFs, is fed into the gap between the rubber roller and the radial cutter. At the following, the CF tow is chopped into short pieces, and chopped CFs are produced. The chopping process of the CF tow mainly consists of two steps. First, the CF tow is chopped by being immerged into the elastic support, as indicated in Figure 1(b). Second, the CF tow is chopped by cutters, as depicted in Figure 1(c). Lastly, the chopped CFs drop out from the bottom surface of the radial cutter. The qualified chopped CFs are shown in a magnified view in Figure 1(a).

Unlike conventional engineering materials, such as steel and plastic, CFs are flexible as well as brittle. Recently, considerable amount of effort has been spent on the properties of CFs and its composites, such as the thermal properties [8,9], tensile properties [10], fracture behavior of CF reinforced composites [11,12]. But there are still few studies focusing on the fracture mechanism of CFs being chopped on the elastic support. In previous studies [7], we investigated the wear patterns and mechanisms of the blade during the manufacturing of PAN-based chopped CFs. Here, we study the fracture behavior of a PAN-based CF tow during the chopping process with an elastic support. The influences on the fracture behavior were tested in the experiments, including radii of the blade edge, hardness of the elastic support and chopping depth. We hope that this paper will be a useful guide for the optimal design of CF chopping procedures and equipment.

*Corresponding author: meluls@scut.edu.cn

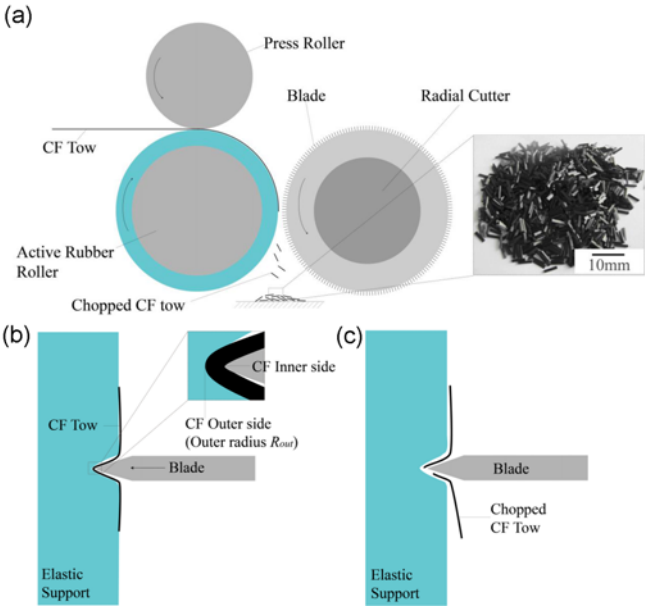

Figure 1. Schematic of radial chopping technology and chopping processes (a) radial chopping technology setup, (b) CF tow chopped into the elastic support, and (c) CF tow chopped by the blade.

Experimental

Experimental Setup

The experimental setup in this work is depicted in Figure 2, including a micro-shift platform, a force sensor, a blade fixture, a blade and a polyurethane (PU) plate, which is used as the elastic support. The micro-shift platform has three separate axes of movement, including *X*, *Y* and *Z*. The blade is fixed on the vertical *Z*-axis (Newport M-VP-25XA) with a moving accuracy of 0.14-0.2 μm and a maximum load of 60 N. The micro-shift platform is controlled by a tri-axial motion controller (Newport ESP301-3N) and a computer with controlling software Newport ESP301. To reduce the effects of the surrounding environments, the micro-shift platform is fixed onto a vibration isolation table (Jiangxi Liansheng Technology Co. ZDT15-09). The force sensor (Kistler 9256C1), which has a sensitivity of -26 pC/N on the *Z*-axis, is used to measure the cutting force in the chopping process. The force sensor is fixed to the moving component of the micro-shift platform by screws and connected to a charge amplifier (Kistler 5080A), data collector (Kistler 5697A) and computer with control software (Dynoware 2825A). The blade fixture (GIN VL10), whose verticality and levelness are both 0.003 mm, is fixed onto the pressure sensor using several screws.

Preparation of the Different Radii of the Blade Edge

The blade is a 25 mm×19 mm×0.9 mm fiber chopping blade in which the rake angle and the back angle are equal,

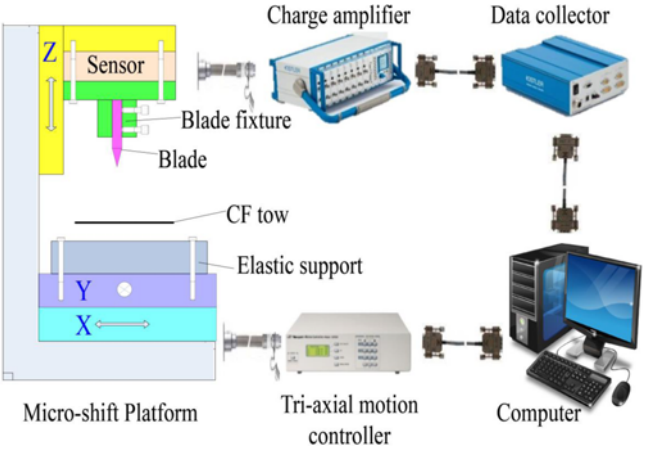

Figure 2. Schematic of the experimental setup.

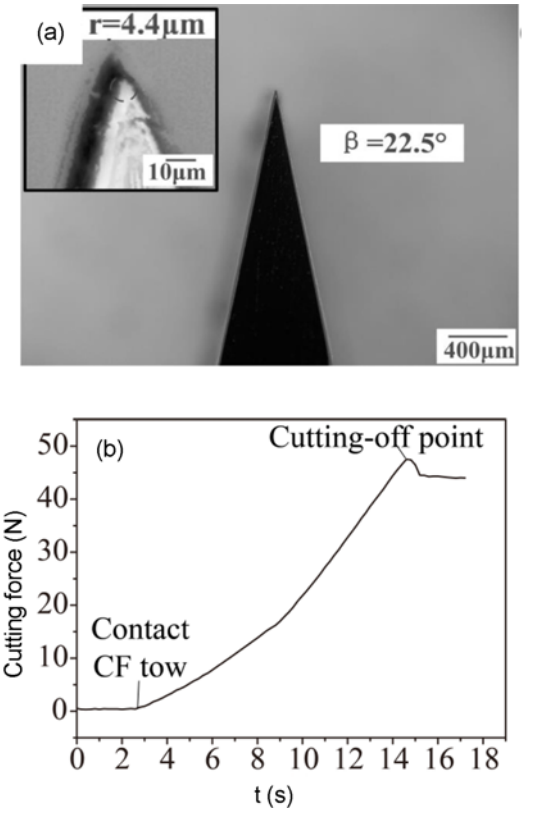

Figure 3. The cutting parameters (a) edge radius and edge angle of the blade and (b) typical cutting force curve of the CF tow.

i.e., so-called edge angle (β). The material of the blade is SK2 die steel, and its quenching hardness is HRC 60-65 °. The edge angle and the cutting edge radius (r) are measured through the blade section image. First, 400-mesh, 600-mesh, 800-mesh and 1200-mesh water-resistant sandpapers were used to polish the blade section. Then, the blade section was polished using a metallographic sample polishing machine with a 1 μm metal polishing agent. Lastly, a super depth

Table 1. Properties of T700SC-12K CF

CF	Monofilaments	Tensile strength (MPa)	Tensile modulus (GPa)	Strain to failure (%)	Linear density (g/1000 m)	Density (g/cm^3)
TORAY T700SC-12K	12×10^3	4900	230	2.1	800	1.8

field microscope (KEYENCE VHX-1000) was used to shoot images of the blade section and measure the β and r values. Blades with different edge radii were prepared by manually polishing with 320-mesh to 800-mesh water-resistant sandpapers in sequence. The resulting blade section image is illustrated in Figure 3(a), where β and r are the average of three repeated measurements.

Carbon Fibers

The experimental CF material used was T700SC-12K (Toray). The properties of T700SC-12K are depicted in Table 1, which is provided by the manufacturer. The width of the CF tow is 6.7±0.2 mm, and the thickness of the CF tow is 0.12±0.01 mm. The results are the averages of five different measured positions, and the standard deviations are the error limits.

Experimental Methods

First, a segment of the CF tow in 100 mm long was cut from the continuous CF tow. Then, the segment was placed flat on the PU plate with its lengthwise direction vertical to the edge of the blade. Next, the blade fed vertically down to the elastic support with a speed of 0.1 mm/s to cut the segment. The cutting force was recorded with a frequency of 100 Hz. Lastly, the cutting edge of the segment, which came into contact with the blade edge, was marked to observe the fracture morphology. To reduce experimental errors, the experiments were repeated five times for each chopping parameter, and the cutting location on the PU plate was changed in each experiment to avoid potential negative effects caused by the damage of the PU.

A typical curve of CF cutting force is depicted in Figure 3(b). Before the blade touches the CF tow, the cutting force keeps zero. Therefore, the mean values of the initial 100 data points are used as background scatter and subtracted. On the cutting force curve, a peak can be clearly observed. A similar peak on the cutting force curve was used as the cutting-off force for a fiber by Moreland [13]. Therefore, the mean value of the peaks deduced from five repetitions was used as the cutting-off force of the CF tow, and the standard deviation was used as the limit of error. In this paper, the cutting depth associated with the cutting-off force is defined as the cutting-off depth (h_0), which can be calculated as follows:

$$h_0 = v(t_2 - t_1) - H \quad (1)$$

where v is the blade feed speed; t_1 is the moment when the cutting force starts to increase; t_2 is the moment associated with the cutting-off force; and H is the thickness of the CF tow.

To avoid any errors caused by different blades, a consistent blade was used in all experiments. As provided by the manufacturer, the blade can be used for more than 10000 times to cut CFs. Because the blade was only used less than 200 times, the tool wear cannot be observed (×100). Moreover, the cutting-off forces of the first experiment (47.362±0.279 N) and the last experiment (47.339±1.732 N), both of which have the same cutting parameters (r=4.4 μm, and the hardness of the PU is 75A), differ slightly, which further indicates that the tool wear has no apparent effect on the experimental results. Hence, the tool wear of the blade was ignored.

Results and Discussion

Failure Order in the CF Tow

To study the fracture behavior of the PAN-based CF tow in the chopping process, the failure order of the CF tow was observed and analyzed. As indicated in the magnitude view in Figure 1(b), the failure order between the inner and outer side of the CF tow was determined by controlling the maximum cutting depth $h_{max.}$

The typical cutting force curves with different h_{max} are illustrated in Figure 4(a), where the zero-time is the moment when the cutting force starts to increase. When h_{max} was 1.1 mm, 1.15 mm and 1.2 mm, the CF tows were completely cut off, and all of the cutting-off forces were similar. When h_{max} was 1.0 mm and 1.05 mm, the CF tows were cut off incompletely, and only certain parts of the CF tow were broken. Figure 4(b) depicts the fracture images of the CF tow when h_{max}=1.05 mm. The fracture width of the CF tow on the inner side, where the blade edge directly contacts with the CF tow, is larger than that on the outer side. Furthermore, a crack appears in the middle of the CF tow inner side whereas no crack occurs in the middle of the CF tow outer side. Furthermore, the fracture width increases with the rise of h_{max}, as indicated in Figure 4(c), where the fracture width is an average of the five repetitions, and the error bar is the standard deviation. All of these results indicate that the fracture process of the CF tow primarily begins from the inner to the outer side and from the tow edge to the tow middle. This process primarily occurs due to the brittle property of CF, whose fracture conforms to Griffith's crack theory [14]. Tensile, compressive and shear strain can lead to a failure point. Because the inner side of the CF tow has the smallest bending radius, the innermost monofilament layer

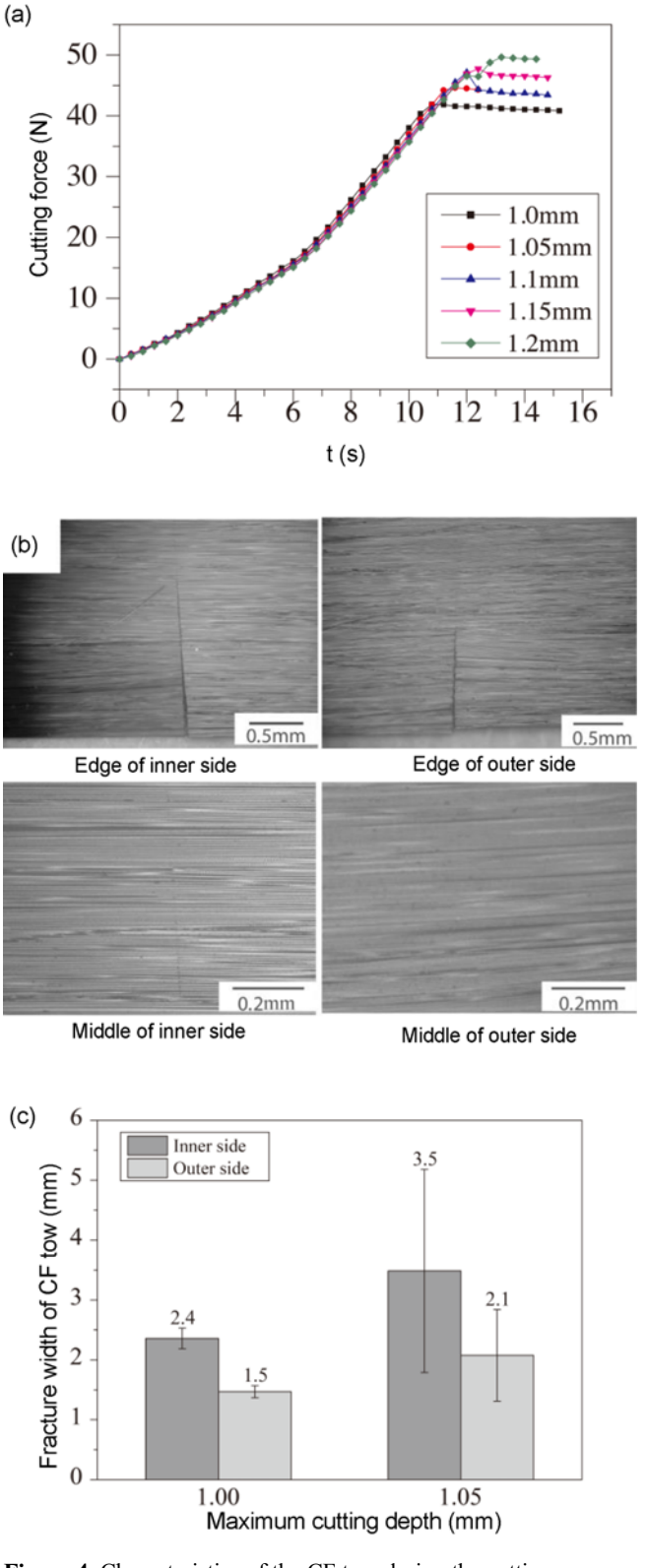

Figure 4. Characteristics of the CF tow during the cutting process with different maximum cutting depths (a) cutting force curves; (b) fracture images of the CF tow when h_{max}=1.05 mm, and (c) fracture width of the CF tow when h_{max} is 1.0 mm and 1.05 mm.

will fracture first.

Effects of the Elastic Support Hardness

In industrial production, the PU hardness typically varies from 70 A to 90 A. To study the elastic support hardness effects on fracture behaviors, five kinds of PU with different hardness were selected as the elastic support, and their detailed hardness and variation distribution are depicted in Figure 5(a). The cutting-off force and cutting-off depth were measured during the experiments, as depicted in Figure 5(b). When the PU hardness increases, there is no clear trend in the cutting-off force. However, the cutting-off depth decreases significantly with the increase of PU hardness, implying that the PU pressure affects more than the cutting depth during the cutting process. Furthermore, the PU pressure depends on the cutting depth. In industrial production, a smaller cutting-off depth is preferred because it results in less vibration of the cutting tool, which will extend the cutting tool life. However, there is a trade-off that a harder PU plate typically signifies a lesser number of available cutting times because of the reduction in fatigue strength. A suitable PU hardness should be selected in industrial production.

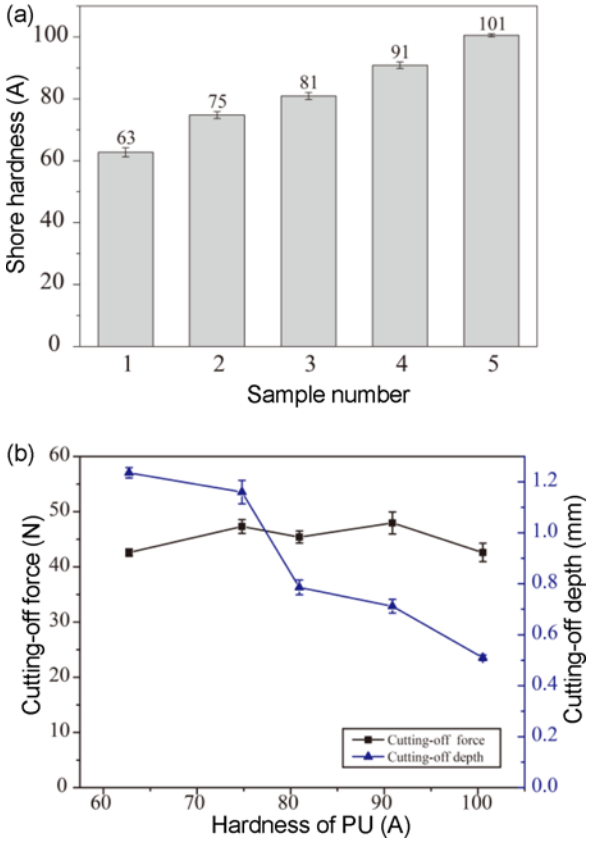

Figure 5. Effects of PU hardness on cutting-off force and cutting-off depth (a) hardness and variation and (b) cutting-off force and cutting-off depth with different support hardness.

Fracture Morphology of the CF Tow Chopping Process

In order to further analyze the fracture mechanism of the PAN-based CF tow in the chopping process with an elastic support, the fracture surface morphologies of the CF tow were observed. It has been proven that CF depicts different fracture surface morphologies in different fracture modes.

The CF fracture surface morphologies in different failure modes have been analyzed by Da Silva *et al.* [15] , Naito *et al.* [16,17], and Lu *et al.* [18]. It was revealed that the fracture surface morphologies are different between tensile, flexure, and shear fracture. The fracture morphologies of the different fracture methods are depicted in Figure 6. Figure 6(a) presents the tensile fracture morphology of a PAN-based CF, in which the fracture surface is flat with a certain degree of roughness. Figure 6(b) illustrates the flexural fracture morphology of the same type of PAN-based CF. Compared with tensile fracture, flexural fracture exhibits a distinct difference in fracture characteristics on the compression side of the PAN-based CF, where the fracture surface exhibits a rugged texture instead of a flat surface. Figure 6(c) illustrates the section image of the CF cut on a glass plate using a blade, and the fracture surface is flat and smooth. Hence, the fracture mode should be different from the former two modes. This result primarily occurs because the shear action plays a vital role in the fracture process instead of the tensile or flexural action. In summary, the tensile, flexural and cut fracture processes can be simplified as Figure 6(d), (e) and (f), respectively.

To reveal the fracture mechanism of the PAN-based chopped CF tow with elastic supports, the fracture surfaces

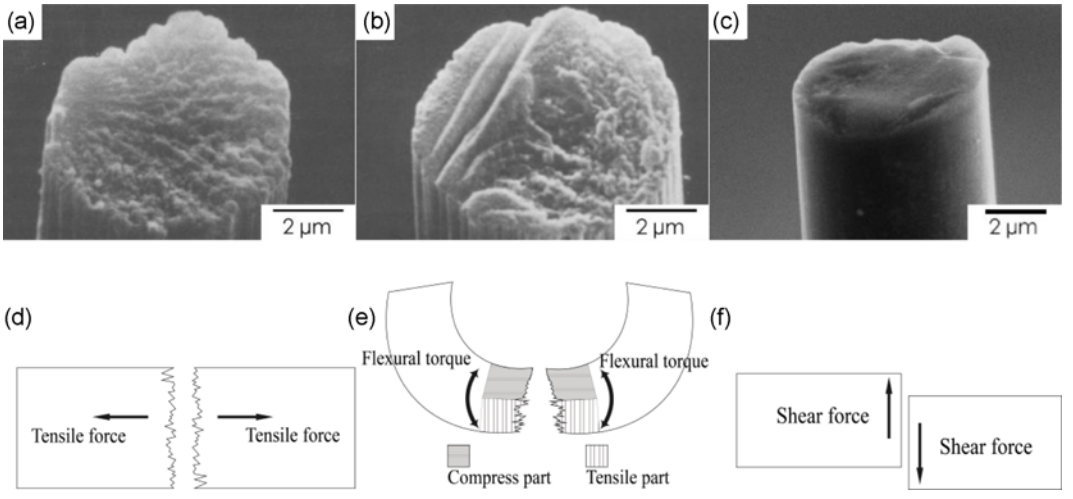

Figure 6. Fracture surfaces of CF filaments of different failures; (a) tensile, (b) flexural, (c) shear, schematic of modes of CF fracture; (d) tensile, (e) flexural, and (f) shear.

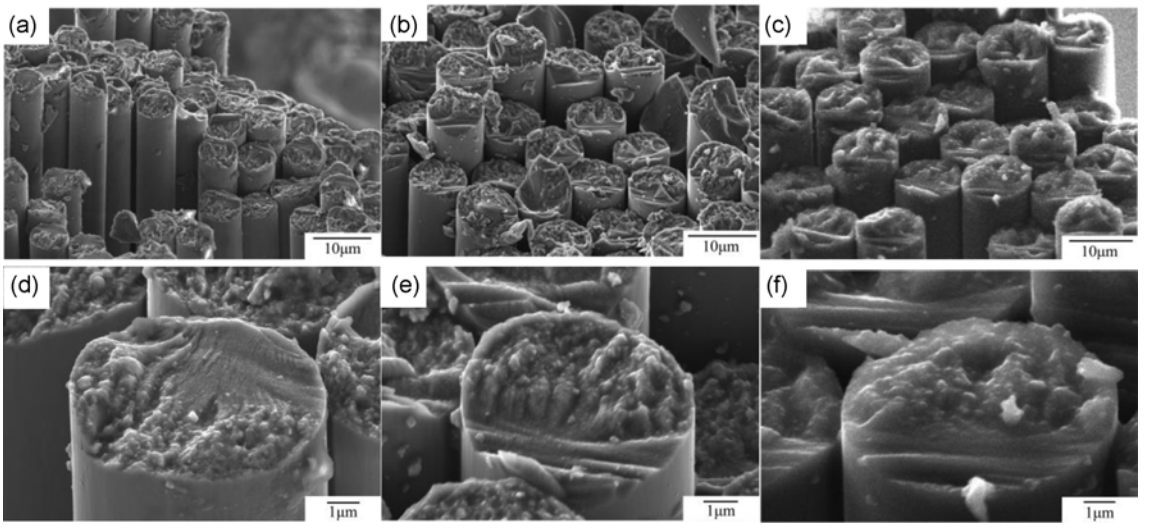

Figure 7. Fracture surfaces of the CF filaments chopped by different blade edge radius (a), (d) r=4.4 μm; (b), (e) r=29 μm; and (c), (f) r=40 μm.

of the CF were observed after cutting with different blade edge radii, as depicted in Figure 7. The fracture characterization of the tensile and compression part appears on most of the filaments, in which most of the filaments were broken because of flexural fracture. It is interesting that we can hardly find one flat fracture surface. This result indicates that when the CF tow is cut on an elastic support, the dominant fracture mode is flexural fracture but not shear fracture. This phenomenon can be explained basing on the cutting conditions. Due to the friction between the CF tow and the elastic support, blade pressure, support force, elastic support strain, the CF tow is applied tensile, shear force and flexural torque simultaneously during being cut into the elastic support. According to the previous work [18], the cutting-off force of a single CF filament on elastic substrate is about 10 mN in flexural fracture mode, while the force is about 244 mN on rigid substrate in shear fracture mode. In the experiments of this work, the cutting-off force of CF tow, who has 12,000 filaments, was about 40 N. This cutting-off force value fits more on the flexural fracture mode according to the value of a single CF filament. Moreover, due to the chopping process lasting a period of time, the cutting-off force of CF-tow is smaller than the scale-up value of a single CF filament. Therefore, the CF tow meets its maximum flexural strength before the maximum tensile and shear strength, so the CF tow exhibits flexural fracture morphologies.

Robustness of the PAN-based CF Chopping Process with an Elastic Support

The cutting-off forces and cutting-off depths generated by the different blade edge radii in the chopping process (PU hardness is 75A) are illustrated in Figure 8(a). When the blade edge radius varies from 4.4 μm to 40 μm, the cutting-off force increases with the increase of blade edge radius. However, there is no significant difference among the cutting-off depths with different blade edge radii. This phenomenon illustrates the robustness of the PAN-based CF chopping process with an elastic support. The cutting depth remains nearly the same when the cutting tool is worn, and the CF tow can continue to be cut off. The explanation for this characteristic can be given as follows:

According to Hooke's law,

$$\sigma = -c\varepsilon \tag{2}$$

where σ is the stress tensor, ε is the strain tensor, c is the stiffness tensor.

In a Cartesian coordinate system for continuous media, the stress and strain tensors can be represented by 3×3 matrices as follows:

$$\sigma = \begin{bmatrix} \sigma_{11} & \sigma_{12} & \sigma_{13} \\ \sigma_{21} & \sigma_{22} & \sigma_{23} \\ \sigma_{31} & \sigma_{32} & \sigma_{33} \end{bmatrix} \tag{3}$$

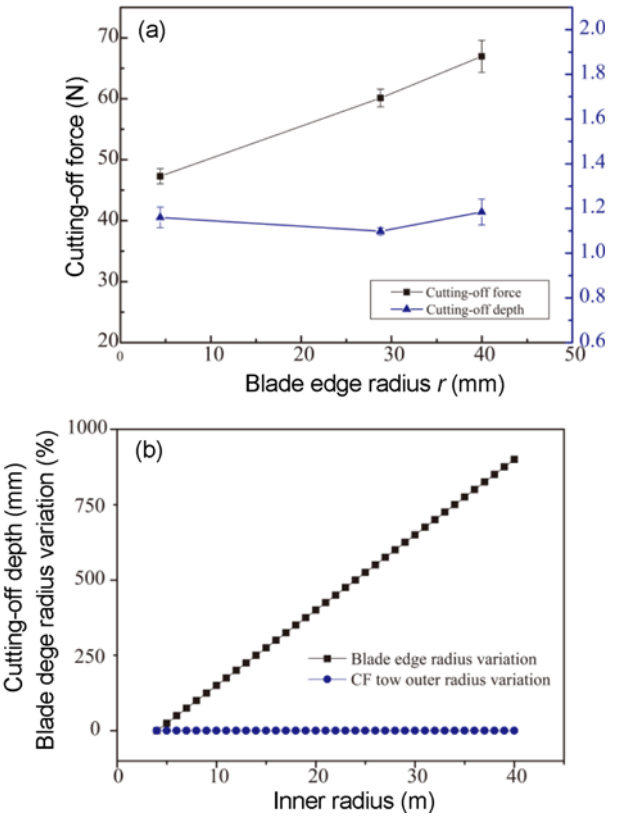

Figure 8. Robustness of the blade edge radius (a) effects of the blade edge radius on the cutting-off force and the cutting-off depth and (b) variation in the blade edge and fiber tow outer-side radius caused by the blade edge radius change.

$$\varepsilon = \begin{bmatrix} \varepsilon_{11} & \varepsilon_{12} & \varepsilon_{13} \\ \varepsilon_{21} & \varepsilon_{22} & \varepsilon_{23} \\ \varepsilon_{31} & \varepsilon_{32} & \varepsilon_{33} \end{bmatrix} \tag{4}$$

c is represented by a 3×3×3×3 matrix. Thus, Hooke's law for continuous media can be expressed as follows:

$$\sigma_{i,j} = -\sum_{k=1}^{3}\sum_{l=1}^{3} c_{ijkl}\varepsilon_{kl} \tag{5}$$

where i and j value 1, 2 or 3.

When the PU plate is cut into a certain depth by a blade with a certain cutting edge angle β and edge radius r, the stress tensor σ remains the same.

When the blade edge is worn, the blade edge radius becomes larger. For the CF tow, the bending radius increases accordingly. Therefore, the stress tensor changes. The stress variation before and after the blade edge wear can be estimated by calculating the outer bending radius of the CF tow.

The outer-side bending radius of the CF tow can be calculated as follows:

$$R_{out} = r + T \quad (6)$$

where T is the thickness of the CF tow, which is 0.12 mm in this study.

Then, the variation in the radius before (r=4 μm) and after (r=4 μm) the blade edge wear can be evaluated, as illustrated in Figure 8(b). Hence, if the blade edge radius changes from 4 μm to 40 μm, the blade edge radius variation is up to 900 % while the fiber tow outer-side radius variation is only 0.3 %. The robustness of the blade edge radius during the cutting process is another indication that the fiber tow failure mode is flexural fracture.

Conclusion

The fracture behavior of a PAN-based CF tow being chopped on an elastic support was studied using an experimental method. Several conclusions can be obtained as follows:

1. The failure mode of the CF tow being chopped on the elastic support is flexural fracture.
2. The CF tow breaks from the bending inner side to the outer side during the chopping process.
3. Because the failure mode of the chopped CF tow is flexural fracture, the PU pressure affects more than the cutting depth during the cutting process.
4. Because the failure mode of the chopped CF tow is flexural fracture but not shear fracture, the chopping structure shows good robustness of the blade radius change.

Acknowledgments

The current study was supported by the National Natural Science Foundation of China (No. U1401249, 51375175), the Natural Science Foundation of Guangdong Province, China (No. 2015A030313201, No. 2014A030312017) and the Science and Technology Planning Project of Guangdong Province, China (No. 2015A010105007). The authors also thank to the Pearl River S&T Nova Program of Guangzhou and the Fundamental Research Funds for the Central Universities.

References

1. E. Frank, F. Hermanutz, and M. R. Buchmeiser, *Macromol. Mater. Eng*., **297**, 493 (2012).
2. W. Dong, H.-C. Liu, S.-J. Park, and F.-L. Jin, *J. Ind. Eng. Chem.*, **20**, 1220 (2014).
3. Z. Wang, K. Li, and C. Wang, *Constr. Build. Mater*., **64**, 288 (2014).
4. F. Ahmad, *J. Mater. Process. Technol*., **169**, 263 (2005).
5. N. G. Karsli and A. Aytac, *Compos. Pt. B-Eng.*, **51**, 270 (2013).
6. C. Ozkan, N. Gamze Karsli, A. Aytac, and V. Deniz, *Compos. Pt. B-Eng.,* **62**, 230 (2014).
7. Z. Shen, L. Lu, J. Sun, F. Yang, Y. Tang, and Y. Xie, *Int. J. Mach. Tools Manuf.*, **97**, 1 (2015).
8. G. Lalet, H. Kurita, J.-M. Heintz, G. Lacombe, A. Kawasaki, and J.-F. Silvain, *J. Mater. Sci*., **49**, 397 (2014).
9. T. Han, H. Wang, X. Jin, J. Yang, Y. Lei, F. Yang, X. Yang, Z. Tao, Q. Guo, and L. Liu, *J. Mater. Sci.*, **50**, 2038 (2015).
10. K. Naito, *J. Mater. Sci.*, **48**, 4163 (2013).
11. T. Lin, D. Jia, P. He, and M. Wang, *Mater. Sci. Eng. A*, **527**, 2404 (2010).
12. S. U. Khan, A. Munir, R. Hussain, and J. K. Kim, *Compos. Sci. Technol*., **70**, 2077 (2010).
13. J. C. Moreland, Ph.D. Dissertation, Clemson Univ., South Carolina, 2010.
14. E. H. Yoffe, *Lond. Edinb. Dubl. Phil. Mag.*, **42**, 739 (1951).
15. J. L. G. Da Silva and D. J. Johnson, *J. Mater. Sci.*, **19**, 3201 (1984).
16. K. Naito, Y. Tanaka, J. M. Yang, and Y. Kagawa, *J. Am. Ceram. Soc.*, **92**, 186 (2009).
17. K. Naito, Y. Tanaka, J. M. Yang, and Y. Kagawa, *Carbon*, **46**, 189 (2008).
18. L. Lu, Z. Hou, F. Zhang, Y. Xie, and Y. Tang, *Text. Res. J.* Doi:10.1177/0040517516654107 (2016).